

Automatic Rock Mass Discontinuities Detection Based on Binocular 3-D Reconstruction

J.Q. Chen ^{a, b}, H.H.Zhu ^{a, b*}, X.J.Li ^{a, b}

^aKey Laboratory of Geotechnical and Underground Engineering of Ministry of Education, Tongji University

^bDepartment of Geotechnical Engineering, Tongji University
* heichenjianqin@163.com(zhuhehua@tongji.edu.cn)

Abstract

Measurement of rock mass discontinuities was the key for rock mass 3D network simulation, seepage analysis, and stability analysis. In this paper, a non-contact rock mass discontinuities detection method based on the single camera binocular three-dimensional reconstruction theory was presented. This method provided an effective way for grouping rock mass discontinuities and calculation the discontinuity orientations. The main flow of the method was: (1) obtaining three dimensional point cloud data based on the binocular three-dimensional reconstruction theory by single camera, (2) de-noising and re-sampling on point cloud data before triangulation to reduce holes in the reconstructed triangular mesh, (3) grouping rock mass discontinuities automatically based on an improved K-means algorithm which adopted density and clustering validity indexes, (4) segmenting the discontinuities in the same group based on the angle and the adjacent relationship between two triangular facets, and (5) fitting the segmented point cloud using the Random Sample Consensus (RANSAC) algorithm and calculating its orientation. This method was applied to the grouping and measurement of discontinuities of a rock mass slope. The results showed that the grouping and measurement of discontinuities were reliable and of high accuracy that could meet the engineering requirements.

Keywords: discontinuity, binocular 3-D reconstruction technique, K-means clustering, grouping, orientation.

1. Introduction

Volumes of rock contain a wide range of ‘planes of weakness’ at all scales, each with a statistical distribution of spacing and orientation (Goodman, 1989). In rock engineering, these planes of weakness are generally referred to as ‘discontinuities’. It is essential to characterize its continuity geometry properties at exposed rock faces in permeability studies for hydrological, mechanical behaviour assessment and in the engineering design of man-made structures placed in or on rock masses.

Geometric properties of discontinuity include trace length, orientation and spacing. The most important discontinuity property is orientation. Orientation influences the potential of the rock mass to move, the direction of movement and the volume of material to be moved (Donovan, 2005).

Traditionally, the orientation measurement technique of a compass-inclinometer relies on a visual inspection and direct measurements by a qualified field engineer. However, the manual method of mapping can be dangerous, time consuming, biased, error prone and limited in their coverage.

More recently, terrestrial laser scanning (Schulz et al., 2005; Dove and Badillo, 2008; Otoo et al., 2011; Gigli and Casagli, 2011; Collins and Stock, 2012; Liu, 2013) and 3D photogrammetry (Roncella et al., 2005; Potsch et al., 2005; Haneberg, 2008; Sturzenegger et al., 2009) with the potential to address all the above problems have been employed. 3D photogrammetry which is triggered by the arrival of high quality and affordable digital cameras can be accomplished with a great deal of flexibility.

The field of automated mapping of geological discontinuities from 3D LiDAR or photogrammetry surface models has been widely researched, published, and presented. Slobet al. (2005) analyzed the 3D mesh and plots the facet orientations in a polar plot to determine the number of discontinuities sets.

Then automatically outline the individual discontinuity sets through fuzzy K-means clustering algorithm. Jaboyedoff et al. (2007) proposed the calculation of the normal vector orientation for every point and its coplanar neighbours using principal component analysis method. Olariu et al. (2008) presented a clustering approach on the raw point cloud data in order to determine discontinuity set orientations. Gigi et al.(2011) searched voxels of space and determines local planarity, from which local discontinuity sets are merged and the associated set orientations are calculated.

This paper proposes a new approach for the automatic identification and extraction of discontinuities. The main novel contributions of the proposed method are: (a) a technique on how to use overlapping photographs to create 3D point clouds using off-the-shelf cameras; (b) automatically extract of discontinuity orientations and discontinuity sets based on an improved K-means algorithm.

2. Obtain 3D point clouds based on a single camera binocular 3-D reconstruction system

Binocular three-dimensional reconstruction technique simulates the human visual mechanism, with two cameras with known internal parameters and external parameters photographed simultaneously to have the stereo pair in order to conduct three-dimensional reconstruction of the surface of the objects. However, the binocular system has fixed shooting angle and baseline length, making it difficult to adapt to the 3D reconstruct of large object. The binocular system based on single camera could compensate for these shortcomings. It used only one camera shot twice in different locations to get the stereo pair. Common points were identified in pairs of overlapping photos, and a bundle adjustment was performed to determine the relative camera locations.

The application of our method to a real case study was carried out in a rock mass slop with well-developed joint at the outlet of the tunnel. A precisely calibrated Canon EOS 5D Mark II camera with a 24-mm long lens was used for this project. Calibration was typically done once for each camera and lens combination. A tripod was used to steady the camera, and a remote switch was used to activate the shutter and minimized movement of the camera. Firstly, choose two shooting positions to get the stereo image pair of rock surface. Then conduct feature point detection and matching to calculate the relative pose of the two shooting. Lastly, perform epipolar rectification and dense matching to acquire the 3D point clouds. The specific process was shown in Figure 2. Point clouds obtained were based on the left camera coordinate system and contained only gray information. So the RGB value of pixel in the left image could be assigned to the corresponding point to have more realistic rock mass point clouds, as shown in Fig. 3.

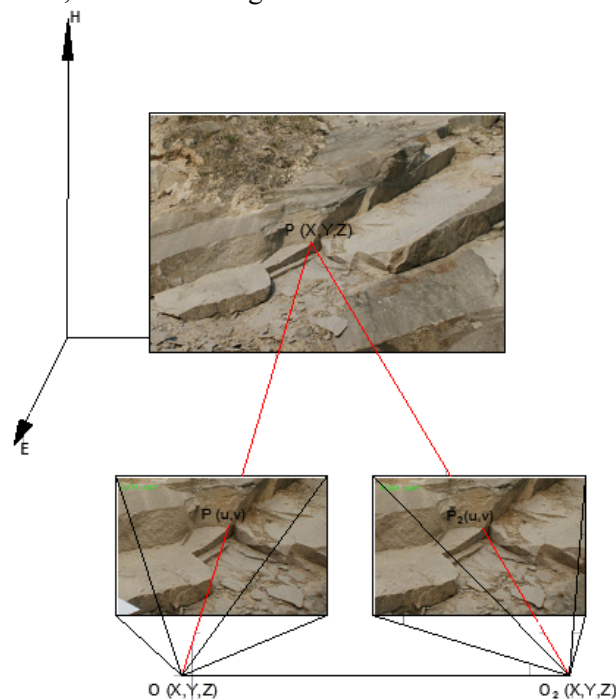


Fig. 1. Sketch of obtaining left and right images

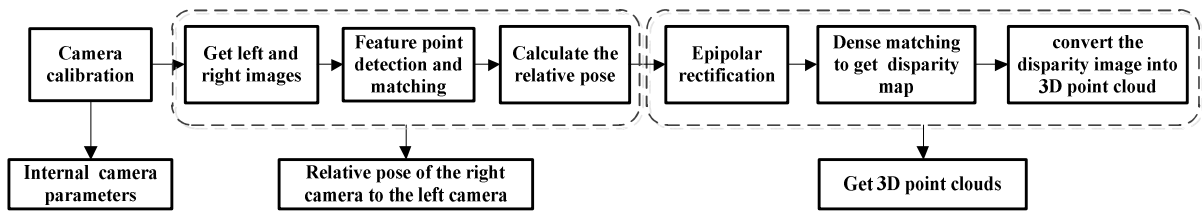


Fig. 2. Flowchart of binocular 3D reconstruction based on single camera

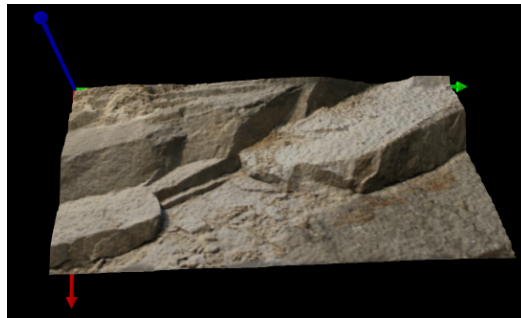


Fig. 3. Figure of 3D point cloud with RGB information

3. Point clouds noise removal and triangulation

After 3D reconstruction, we could obtain point clouds of rock mass slop (110073 points). Perform triangulation of point clouds to obtain the topological relations between point clouds. The meshed surface was stored as a list of vertices and a list of facets. The vertex list contained the x, y and z coordinates of all the corner points of the facets.

3.1 Point clouds noise removal

The point clouds obtained through 3d reconstruction were very dense and contained a lot of noise. If they were triangulated directly, the triangulation would have many holes and overlaps. In this paper, Moving Least Squares method (MLS) (Alexa and Behr, 2003) was used to remove noise. Figure 4 (a) was not de-noising before triangulation. Figure 4 (b) was de-noising before triangulation. Contrast Figure 4 (a) and 4 (b), after removal of noise, mesh was smoother and contained lesser holes.

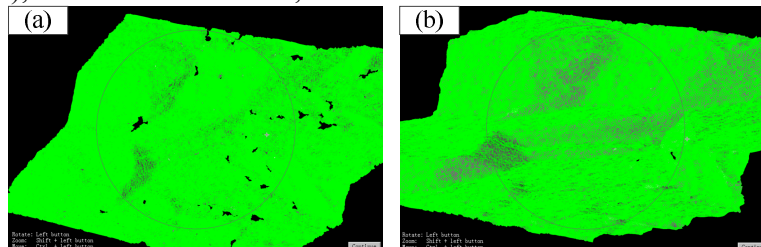


Fig. 4. Comparison chart of triangulation with or without de-noising (a) de-noise before triangulation; (b) triangulation without de-noising

3.2 Point clouds resample

Because the 3D reconstructed point clouds were very dense and lost local information, they need to be resampled. On one hand, it could reduce the point clouds density, reducing the number of triangular facets, improving triangulation and clustering analysis speed; On the other hand, it could repair and recover the geometric details of point clouds model.

3.3 Triangulation

Perform triangulation for point clouds using Greedy Triangulation algorithm provided by Halcon software (MVTec, 2008) and save the triangulation results into the polygon model as PLY file format. Then import this file into MATLAB and read triangular mesh vertices and faces information to prepare for subsequent clustering analysis.

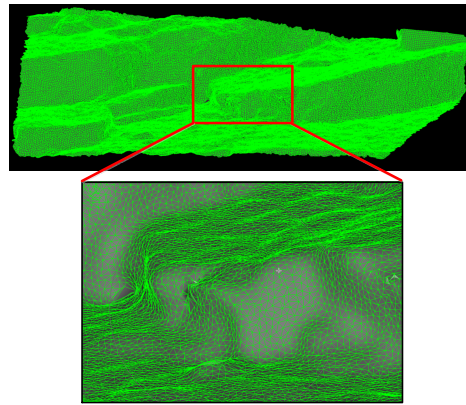


Fig. 5. Figure of triangulation

4. Automated grouping of discontinuities

After the reconstruction of the rock surface in a 3D mesh, the surface mesh could be analyzed. The surface mesh consisted of triangles, also called facets. These three corner points uniquely defined the orientation of the facet, similar to the way orientations of discontinuity planes were defined. The key point of automated grouping of discontinuities was to perform cluster analysis for these small triangular patches. Automated grouping process used in this paper was shown in Fig. 6.

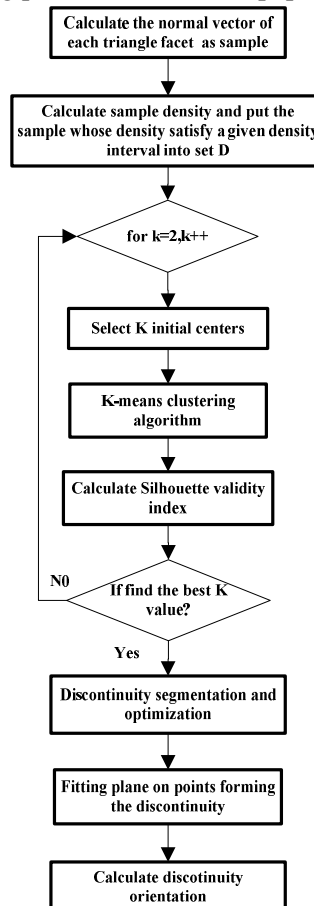


Fig. 6. Algorithm flowchart of automatic grouping of rock mass

4.1 Basic definitions

Clustering analysis of triangular facets was based on the normal vector orientation of triangular patches. Therefore, the three-dimensional space coordinates of triangular facets (three vertices coordinate of triangular face) were recalculated to extract the unit normal vector. The unit normal vectors of each triangular facet were treated as the sample to be clustering, which could effectively reduce the complexity of the algorithm.

Sample distance was defined as the angle between the unit normal vectors. Sample density was defined as the number of normal vectors whose sample distance with respect to the given sample was less than a certain angle.

4.2 Improved K-means algorithm based on sample density and clustering validity index

The traditional K-means clustering algorithm assumed that the number of clusters(K) was known, and randomly selected initial centers. Because of only taking the distance factor into consideration, the algorithm often chose many isolated points as initial cluster centers, which could often obtain local optimum results. In view of this, the improved K-means algorithm based on expectation of density and Silhouette validity index was used to group the samples. It took into account both the sample density and sample distance which could effectively improve the selection of initial cluster centers to avoid falling into local optimum. Meanwhile, the algorithm could automatically analyze the clustering quality in different K values and determine the optimal number of clusters by selecting the average Silhouette validity index.

4.2.1 Choose the initial clustering centroids and K values

The key of the algorithm was to select the initial clustering centres and K values.

(a) Select the initial centres

Calculate the density of each sample. Put the sample of which the density was within the setting interval [Min, Max] into the set D. The maximum in the set D was taken as the initial centre and was deleted from set D. Select a sample in set D whose average distance with the selected initial centres was the maximum as a new added initial centre. Likewise, delete this sample from set D. Then, use the same method to choose the rest initial centres until selecting to K centres.

(b) Determine the number of clusters(K)

Assume that the sample set consisted of N clusters C_i ($i=1,2,\dots,N$). Take any object x_i in the set, and denote by C_i the cluster to which it has been assigned. Then $a(x_i)$ was defined as average distance of x_i to all other objects of C_i . And $b(x_i)$ was defined as the minimum of the average distance of x_i to all objects of any cluster which was different from C_i . Use Silhouette validity index to select the optimal K value (Donovan, 2005), which was defined as follows:

$$S(x_i) = \frac{b(x_i) - a(x_i)}{\max\{a(x_i), b(x_i)\}} \quad (1)$$

When the within dissimilarity $a(x_i)$ was smaller than the 'between' dissimilarity $b(x_i)$, a larger $S(x_i)$ could be obtained. That is to say, x_i had been assigned to an appropriate cluster. The Silhouette provided an evaluation of clustering validity, and could be used to select an appropriate number of clusters.

In this paper, K started at 2 and was increased by 1, the average Silhouette index of each K was calculated at the same time. The optimal value K_{opt} satisfied: $S(k_{opt}-1) < S(k_{opt})$, $S(k_{opt}) > S(k_{opt}+1)$. The relatively greater average Silhouette value of the corresponding K value was selected as the final number of clusters.

4.2.2 Automation grouping results

When K was 3, the average Silhouette validity index was the maximum. So rock mass slope could be divided into 3 discontinuity sets. However, there were noisy points in the left corner of the 3D mesh caused by vegetation. These blobby parts would change the orientation of the facets, and therefore these facets would be assigned to other sets. The facets of the 3-D surface could in turn be coloured according to the set number, the digital rendering of which was shown in Fig.7.

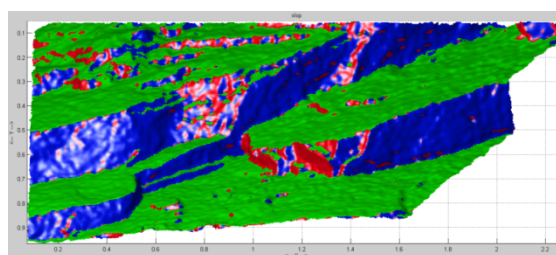


Fig. 7. Visualisation of the effect of the clustering on the 3-D surface

4.3 Classification of facets and vertices to planes

It was assumed that connecting facets that belong to the same discontinuity set were part of the same discontinuity plane. Discontinuity planes within each set were found by connecting neighbouring facets of the same set. Two facets that shared two vertices was the definition of connecting facets that was used. The neighbours of these neighbours were in turn found until all connecting facets were joined into a single plane. Then a re-classification of facets into discontinuity planes was done. The classification was a unique combination of set and plane number. The facets of the 3D surface could in turn be coloured according to the plane number, the digital rendering of which was shown in Fig.8.

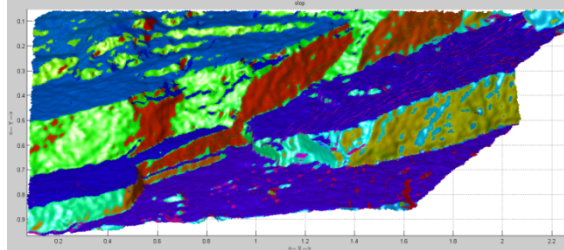


Fig. 8. Visualisation of rock mass segmenting after clustering

4.4 Optimization of the classification result

Because the discontinuities were curved and undulating, the normal vectors of the facets in the concave and convex regions of the 3D surface changed dramatically. It would generate many patches clustered only based on the normal vectors of the facets, as was showed in Fig.8. Therefore, the classification results need to be optimized. The optimization principles were: If the total number of facets in each plane was less than a given threshold, these planes could not exist as independent planes and were extracted to reassign their facets to other independent planes according to their neighbouring relationships. Fig.9 was the visualisation of rock mass segmenting after optimization.

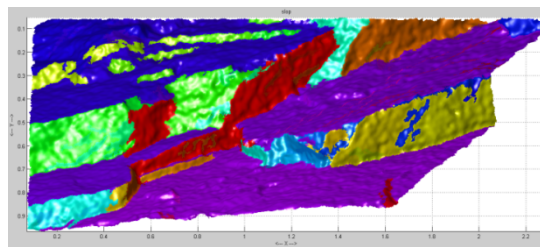


Fig. 9. Visualisation of rock mass segmenting after optimization

4.5 Plane fitting

After the classification of vertices to planes, neighbouring triangles that had similar orientations could be combined into so-called patches to form discontinuity surface. A fracture surface exposed at rock faces was usually rough and wavy. So, orientation of a fracture was actually took as the orientation of its best-fit plane. The computation of the best fit plane could use for example a least-squares method, principal component analysis, Hough transform or Random Sample Consensus (RANSAC) algorithm. RANSAC algorithm took the volatility of the points into consideration would result in a better estimate of the discontinuity orientations (Zhou et al., 2011). Fig.10 was the visualisation of the fitted planes in 3D. Then the plane equation parameters of the individual discontinuity planes could be calculated.

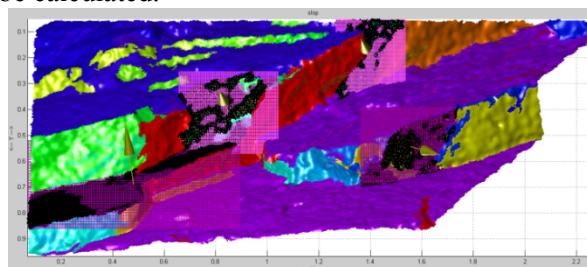


Fig. 10. Sketch of RANSAC plane fitting

4.6 Coordinate transformation

The point clouds of rock mass obtained through binocular three-dimensional reconstruction system was in the left camera coordinate system. But dip direction and dip angle of the discontinuity could only be described in a real world coordinate system. Therefore, the point clouds need to be converted to world coordinate.

This process involved three coordinate systems: World coordinate system (WCS), Camera coordinate system (CCS), Rectified camera coordinate system (RCS). CCS and RCS could be determined by camera internal parameters and camera internal parameters before and after epipolar rectification respectively. The CCS was defined as such that its x and y axes were parallel to the column and row axes of the image, respectively, and the z axis was perpendicular to the image plane and was oriented such that points in front of the camera had positive z coordinates. Coordinate transformation included scale transformation, translation transformation and rigid transformation. Scale and translation transformation did not influence the results of orientation measurement. Therefore, consider only the rotation transformation between the coordinate systems.

In this paper, first calculate the normal of the discontinuity in the camera coordinate and convert it to the world coordinate system to calculate the orientation. Transformation relation between camera coordinate system and world coordinate system was called the camera pose parameter. In this paper, the camera pose acquisition method proposed by Zhou Chunlin (2010) was used.

4.7 Comparison of the novel methods and the traditional method for rock fracture mapping

Select the 6 obvious discontinuities in the scene (indicated with a red circle in Fig.11) and measure the dip direction and dip angle of the discontinuities manually using a geological compass. The orientation of platform extended plane was $230^{\circ} \angle -7^{\circ}$, through which we could calculate the rotation matrix between the left camera coordinate system and the world coordinate.

Then fit six discontinuities plane (marked by red circles) by RANSAC algorithm for the small triangles on each discontinuity after segmentation, as was shown in Fig.12. Calculate the normal vectors of the discontinuities and transform them to the world coordinate system to calculate orientation.

We could see from table 3 that for the dip direction measured by binocular system, the maximum error was 12.4 and the mean error was 6.7. The maximum error was 7.8 and the mean absolute error was 3.6 for the dip angle measurement results.

The discontinuity surface was curved or undulating, however, the occurrence measured by geological compass could only indicate the regional characteristic of discontinuity which could not be representative because it would be influenced by the roughness. Using RANSAC algorithm for plane fitting could take into account the ups and downs of the whole discontinuity as was shown in Fig 12 that the fitted plane passed through the middle of the segmented 3D point clouds. Dip direction measurement result by binocular system was more close to the geological compass when compared to dip angle.

Table 1 Comparison of the occurrence measurement of rock mass.

PN*	Manual*		Binocular* reconstruction		Error*	
	DD	DA	DD	DA	$\Delta DD $	$\Delta DA $
1	239	34	226.6	37.2	12.4	3.2
2	209	87	210.8	84.5	1.8	2.5
3	235	34	225.7	32.8	9.3	1.2
4	230	30	239.9	30.3	9.9	0.3
5	186	63	191.5	70.8	5.5	7.8
6	228	37	226.5	30.5	1.5	6.5

* PN=Number of discontinuities. DD=Dip Direction, DA=Dip Angle, both the unit of dip direction and dip angle was " $^{\circ}$ ". $\Delta|DD|$ =absolute value for deviation of dip direction between manual method and Binocular reconstruction method. $\Delta|DA|$ =absolute value for deviation of dip angle between traditional manual method and Binocular reconstruction method.



Fig. 11. Discontinuities measured with compass

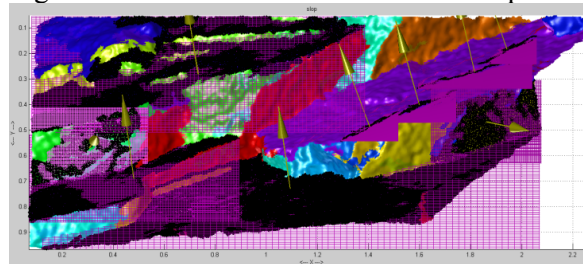


Fig. 12. Sketch of plane fitting.

5. Conclusions

This paper presented an improved K-means algorithm based on sample density and clustering validity index to conduct cluster analysis for the triangulation of the rock mass in order to achieve the automatic calculation of rock mass discontinuities.

The following conclusions could be drawn by measuring the actual rock mass discontinuities.

(1) Point clouds with relatively high accuracy could be obtained through the 3D reconstruction technology based on single camera. Automatically group discontinuities through improved K-means algorithm based on sample density and clustering validity index to conduct cluster analysis. The experimental result showed that the improved K-means algorithm had the advantages of fast convergence speed which was suitable to analyse mass point clouds. Meanwhile, the new algorithm could automatically analyse the clustering quality in different K values and determine the optimal number of clusters by selecting the relatively greater average Silhouette validity index.

(2) For the small triangles in the same set, we could segment them into single discontinuity according to the adjacent relations of the triangles and angle between neighbouring triangles. Use RANSAC algorithm for finding a plane fitting to the triangles in the same discontinuity which could take the uneven property of the whole discontinuity into consideration to get more accurate result. Lastly, through the camera pose parameter measured during shooting, normal vectors in the camera coordinate could be converted to the world coordinate system to calculate the orientation. In this way, we could not only automatically group the rock mass but also measure any discontinuity through non-contact method. The measurement results of discontinuities were reliable and of high accuracy that could meet the engineering requirements.

References

- Alexa M, Behr J, Cohen-Or D, et al. Computing and rendering point set surfaces[J]. *Visualization and Computer Graphics*, IEEE Transactions on, 2003, 9(1): 3-15.
- Collins B D, Stock G M. Lidar-based rock-fall hazard characterization of cliffs[J]. *GeoCongress 2012*, 2012: 3021-3030.
- Dudoit S, Fridlyand J. A prediction-based resampling method for estimating the number of clusters in a dataset[J]. *Genome biology*, 2002, 3(7): research0036.
- Dove J E, Badillo B E, Decker J B, et al. Remote characterization of rock exposures using terrestrial LIDAR[J]. *Proc. of GeoCongress*, 2008.
- Donovan S, Kemeny J, and Handy J, "The application of three-dimensional imaging to rock discontinuity characterization," *Alaska Rocks*, 2005.
- Haneberg W C. Using close range terrestrial digital photogrammetry for 3-D rock slope modeling and discontinuity mapping in the United States[J]. *Bulletin of Engineering Geology and the Environment*, 2008, 67(4): 457-469.

- Jaboyedoff M, Metzger R, Oppikofer T, et al. New insight techniques to analyze rock-slope relief using DEM and 3D imaging cloud points: COLTOP-3D software[C]//*1st Canada-US Rock Mechanics Symposium*. American Rock Mechanics Association, 2007.
- Liu Q. Remote sensing technologies in rock mass characterization[J]. *Rock Characterisation, Modelling and Engineering Design Methods*, 2013: 205.
- MVTEC Software GmbH. *HALCON 9.0*[DB/CD]. Munich, Germany: 2008.
- Goodman. R.E., 1989. *Introduction to rock mechanics. Second edition*. New York etc.: Wiley & Sons, 1989. - 562 p.
- Gigli G, Casagli N. Semi-automatic extraction of rock mass structural data from high resolution LIDAR point clouds[J]. *International Journal of Rock Mechanics and Mining Sciences*, 2011, 48(2): 187-198.
- Otoo J N, Maerz N H, Duan Y, et al. LiDAR and optical imaging for 3-D fracture orientations[C]//*2011 NSF Engineering Research and Innovation Conference*, Atlanta, Georgia. 2011.
- Olariu M I, Ferguson J F, Aiken C L V, et al. Outcrop fracture characterization using terrestrial laser scanners: Deep-water Jackfork sandstone at Big Rock Quarry, Arkansas[J]. *Geosphere*, 2008, 4(1): 247-259.
- Potsch M, Schubert W, Gaich A. Application of Metric 3D Images of Rock Faces For the Determination of the Response of Rock Slopes to Excavation[C]//*ISRM International Symposium-EUROCK 2005*. International Society for Rock Mechanics, 2005.
- Roncella R, Forlani G, Remondino F. Photogrammetry for geological applications: automatic retrieval of discontinuity orientation in rock slopes[C]//*Electronic Imaging 2005*. International Society for Optics and Photonics, 2005: 17-27.
- Slob S, van Knapen B, Hack R, et al. Method for automated discontinuity analysis of rock slopes with three-dimensional laser scanning[J]. *Transportation Research Record: Journal of the Transportation Research Board*, 2005, 1913(1): 187-194.
- Schulz T, Lemy F, Yong S. Laser scanning technology for rock engineering applications[J]. *Optical 3-D Measurement Techniques VII (Eds.: Grün, Kahmen)*, Austria, 2005: 50-59.
- Sturzenegger M, Stead D, Beveridge A, et al. Long-range terrestrial digital photogrammetry for discontinuity characterization at Palabora open-pit mine[C]//*Third Canada-US Rock Mechanics Symposium*. Paper. 2009, 3984.
- Zhou C L, Zhu H H, Li X J. Research and application of robust plane fitting algorithm with RANSAC[J]. *Computer Engineering and Applications*, 2011, 47(7): 177-179.
- Zhou C L, Zhu H H, Zhao W. Non-contact measurement of rock mass discontinuity occurrence with binocular system [J]. *Chinese Journal of Rock Mechanics and Engineering*, 2010, 29(1): 111-117.